



Synthesis and amelioration of inflammatory paw edema by novel benzophenone appended oxadiazole derivatives by exhibiting cyclooxygenase-2 antagonist activity

Naveen Puttaswamy^{a,b}, Vikas H. Malojiao^c, Yasser Hussein Eissa Mohammed^a, Ankith Sherapura^c, B.T. Prabhakar^c, Shaukath Ara Khanum^{a,*}

^a Department of Chemistry, Yuvaraja's College, University of Mysore, Mysore, 570005 Karnataka, India

^b Department of Chemistry, JSS College of Arts, Commerce & Science, Ooty Road, Mysore, 570025, India

^c Molecular Biomedicine Laboratory, Postgraduate Department of Studies and Research in Biotechnology, Sahyadri Science College (Autonomous), Kuvempu University, Shivammogga, 577203, Karnataka, India



ARTICLE INFO

Keywords:

Angiogenesis
Benzophenones
Inflammatory
Oxadiazoles

ABSTRACT

Ten new 2(4-hydroxy-3-benzoyl) benzamide-5-phenyl-1,3,4-oxadiazole derivatives (**10a–j**) were synthesized by coupling 3-benzoyl-4-hydroxybenzoic acid (**5**) with 2-amino-5-phenyl-1,3,4-oxadiazoles (**9a–j**). The structures of these compounds were confirmed by IR, ¹H, ¹³C NMR, and mass spectra, and also by elemental analyses. The anti-inflammatory activity of the compounds **10a–j** were investigated by screening them against human red blood cells (HRBC) *in-vitro*. The results reveal that among this series, compound **10j** with hydroxy substituent, particularly at the ortho position of the phenyl ring attached to the 5th carbon atom of the oxadiazole ring possess significant membrane stabilizing activity in comparison with the control. Further, *in-vivo* chick chorioallantoic membrane (CAM) and rat corneal anti-angiogenesis assays were performed to assess the effect of compound **10j** on endothelial cell migration. This confirmed that compound **10j** inhibits the proliferation of endothelial cells. Anti-inflammatory studies detected the amelioration of carrageen induced rat hind paw edema. Further *in-vivo* and *in-silico* approaches revealed the inhibition of inflammatory marker enzyme cyclooxygenase-2 (Cox-2) and myeloperoxidase (MPO). The study reports that the compound **10j** effectively act against the inflammatory mediated anti-angiogenic disorders which could be translated into a new drug in future.

1. Introduction

Inflammation is a part of the multifaceted biological response of vascularised tissues to damaging stimuli. It is well thought-out as a homeostatic response intended to destroy or deactivate invading pathogens, eliminate squander and debris, that leads to re-establishment of normal function, either through a resolution or restore mechanism [1]. Angiogenesis is considered as a vital constituent of inflammation and its resolution and both are inter reliant events [2]. Some pattern of inflammation, notably chronic inflammation, can encourage vessel augmentation. New vessels may add to a tissue's altered inflammatory reaction [2]. Angiogenesis and inflammation, however, remain distinct cellular events that can come about independently. Many chief transcription factors, such as nuclear factor kappa B, signal transducers and activators of transcription, the vital mediators of inflammatory signaling. Mutually, these transcription factors converge and regulates inflammatory pathways [3]. Molecular events related to these processes

include the activation of downstream molecules such as prostaglandins (PGs) which act as local intermediaries of inflammation which is regulated by cyclooxygenases (COXs). The COX-1 isoform is expressed constitutively whereas COX-2 expression is encouraged during specific pathophysiological conditions or in response to inflammatory stimuli [3]. Another prime hallmark enzyme in the inflammatory response is myeloperoxidase (MPO) mainly secreted by activated neutrophils, portrayed to exhibit powerful pro-oxidative and proinflammatory properties and likely to facilitate the angiogenic gene regulation [4]. Blockage of chronic inflammation may be likely to constrain angiogenesis where the stimulus for vascular growth is consequent from inflammatory cells [5]. Some anti-inflammatory agents may also have anti-angiogenic role that is independent of its effects on inflammation, which add up the fact that agents that have been designed to specifically inhibit angiogenesis may also inhibit chronic inflammation [6].

Benzophenone based analogue is known to exhibit a broad range of biological activity. Primarily, it acts as target specific anti-angiogenic

* Corresponding author.

E-mail address: shaukathara@yahoo.co.in (S.A. Khanum).

pharmacophores which is in the processes of drug development progression [7–10]. On the other hand now a days an increasing interest towards the oxadiazole ring system has been observed as it is the basis for the development of many drugs with a diversity of biological activities. Substituted 1,3,4-oxadiazoles have revealed varied pharmacological activities that include anti-bacterial [11], anti-mycobacterial [12], anti-fungal [13], anti-inflammatory [14], analgesic [15], anti-convulsant [16] and anti-cancer [17] properties. Recently our research group [7,9] has demonstrated that compounds containing oxadiazole moiety induces cytotoxicity and antiproliferative effect on various cancer cell lines and anti-angiogenic potential. With a focused interest in developing a new drug which can specifically target inflammatory angiogenesis disorder, here we hybridized benzophenone with oxadiazole moiety which is reported as having anti-angiogenic potency [9] with an amide linkage. Based on the aforementioned findings and docking-simulated interaction we have made an emphasis that among these newly synthesized series, the compound **10j** emerged as a pharmacological active component particularly inhibiting the COX-2 activity.

2. Result and discussion

2.1. Chemistry

The 3-benzoyl-4-hydroxybenzoic acid (**5**) were synthesized as represented in [Scheme 1](#). Primarily, methyl-4-hydroxybenzoate (**2**) was obtained by esterification of 4-hydroxybenzoic acid (**1**) with methanol in the presence of catalytic amount of sulfuric acid. Then, compound **2** was benzoylated using benzoyl chloride in the presence of dichloromethane (DCM) and triethylamine (TEA) as a base to achieve methyl-4-(benzoyloxy)benzoate (**3**). Further, methyl-3-benzoyl-4-hydroxybenzoate (**4**) was obtained by Fries rearrangement of compound **3** and compound **5** was achieved by the hydrolysis of compound **4** with 10% sodium hydroxide. Besides, 1-benzylidenesemicarbazide derivatives (**8a–j**) were synthesized by reaction of semicarbazide hydrochloride (**6**) with substituted benzaldehydes (**7a–j**) in the presence of sodium acetate. Further, 2-amino-5-phenyl-1,3,4-oxadiazole derivatives (**9a–j**) were obtained by oxidative cyclization of corresponding 1-benzylidenesemicarbazide derivatives using chloramine T (CAT) [18] as represented in [Scheme 2](#).

Finally the title compounds 2(4-hydroxy-3-benzoyl) benzamide-5-phenyl-1,3,4-oxadiazoles (**10a–j**) were achieved as outlined in [Scheme 3](#), by acid amine coupling of compound **5**, with compounds (**9a–j**) in the presence of 1-[bis(dimethylamino)methylene]-1H-1,2,3-triazolo[4,5-b]pyridinium 3-oxidhexafluorophosphate, *N*-[(dimethylamino)-1H-1,2,3-triazolo-[4,5-b]pyridin-1-ylmethylene]-*N*-methylmethanaminium hexafluorophosphate *N*-oxide (HATU) and TEA [19].

All the synthesized compounds were characterized by IR, NMR and mass spectral studies. For example, the IR spectrum of methyl-4-hydroxybenzoate (**2**) showed the presence of O–H stretching at 3312–3490 cm^{-1} , a band for C=O stretching of OCOCH_3 at 1672 cm^{-1} and a signal for C–O stretching at 1210 cm^{-1} . Whereas in ^1H NMR spectrum a signal at 3.8 ppm as a singlet for CH_3 , protons, a multiplet around 6.8–7.9 ppm for aromatic protons and a broad signal at 5.8 ppm for hydroxy proton indicates the formation of compound **2**. However, the formation of methyl-4-(benzoyloxy)benzoate (**3**) was confirmed by

the disappearance of a broadband between 3312–3490 cm^{-1} for phenolic OH of compound **2** and the appearance of a band at 1725 cm^{-1} for C=O of OCOPh in the IR spectrum. Further, the disappearance of a broad singlet at 5.8 ppm of the OH group of compound **2** and increase in the number of aromatic protons in the NMR spectrum clearly indicates, the formation of compound **3**. Similarly the appearance of a band at 3328–3403 cm^{-1} for the OH group in IR spectrum and the presence of a broad singlet at 9.1 ppm for OH group and decrease in the number of aromatic protons in ^1H NMR spectrum indicates the formation of methyl-3-benzoyl-4-hydroxybenzoate (**4**). Wherein the formation of 3-benzoyl-4-hydroxybenzoic acid (**5**) was confirmed by the presence of the band at 3450–3475 cm^{-1} for OH of COOH in IR spectrum and a broad singlet at 12.8 ppm for COOH group and also by the disappearance of a peak at 2.9 ppm for CH_3 protons of compound **4** in ^1H NMR spectrum.

Among the series **10a–j**, 2(4-Hydroxy-3-benzoyl) benzamide-5-(phenyl) 1,3,4-oxadiazole (**10a**) has been taken as a representative example to discuss spectral characterization. In the IR spectrum of compound **10a** the disappearance of a band at 3450–3475 cm^{-1} for COOH of compound **5** and appearance of a band at 3600 cm^{-1} for NH group, similarly disappearance of a singlet at 12.8 ppm for COOH proton of compound **5**, appearance of a signal at 8.1 ppm for N–H proton and increase in the number of aromatic protons in NMR spectrum clearly indicate the acid amine coupling and the formation of compound **10a**.

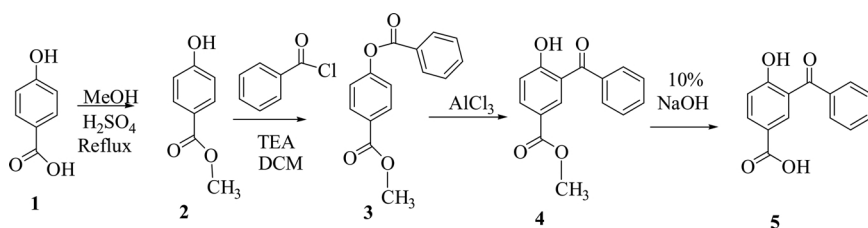
2.2. Biology

2.2.1. Compound **10j** emerged as a lead molecule

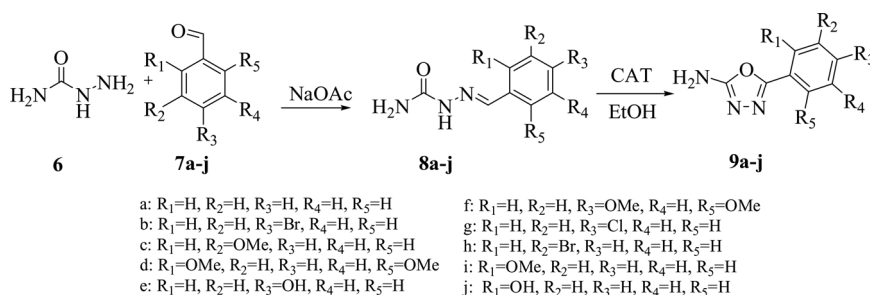
The erythrocyte haemolysis assay is considered as a simple and rapid tool for screening of drugs for anti-inflammatory activity. Most of the anti-inflammatory drugs stabilize the plasma membrane of mammalian erythrocytes and thereby inhibit the hypotonicity induced haemolysis. The plasma membrane of mammalian erythrocytes have been chiefly used as a model to study membrane stabilizing activity of the compounds **10a–j** [20]. *In vitro* anti-inflammatory activity (HRBC membrane stabilization) was performed by increasing concentration (0, 50, 100, 150, 200, 250 $\mu\text{g}/\text{ml}$) of the title compounds **10a–j**. The result demonstrated that compound **10j** bearing hydroxy substitution, particularly at the ortho position of the phenyl ring attached to the 5th carbon atom of the oxadiazole ring possesses significant membrane stabilizing activity compared to the control group and hence selected as a lead compound. The inhibitory concentration (IC_{50}) value of compound **10j** is 153.43 $\mu\text{g}/\text{ml}$ and for the standard indomethacin it is 121.68 $\mu\text{g}/\text{ml}$, ([Table 1](#)). Based on the IC_{50} values, compound **10j** was chosen as a lead compound.

2.2.2. Structure activity relationship (SAR) and selection of **10j** as a potent anti-inflammatory and anti-angiogenesis agent

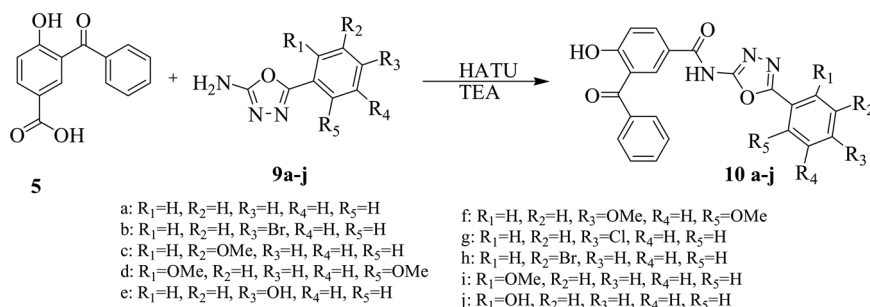
The present study was carried out to evaluate the biological significance of synthesized benzophenone embedded oxadiazole analogues **10a–j**. Based on HRBC membrane assay, among the series **10a–j**, the compound **10j** has exhibited a potent inflammatory angiogenesis activity with IC_{50} 153.43 $\mu\text{g}/\text{ml}$. From this study it is interesting to note that the presence of hydroxy substitution, particularly at the ortho position of the phenyl ring attached to the 5th carbon atom of the



Scheme 1. Synthesis of 3-benzoyl-4-hydroxybenzoic acid (**5**).



Scheme 2. Synthesis of 2-amino-5-phenyl-1,3,4-oxadiazoles (9a-j).



Scheme 3. Synthesis of 2(4-Hydroxy-3-benzoyl) benzamide-5-(phenyl) 1,3,4-oxadiazole (10a-j).

oxadiazole ring, exhibited a good anti-inflammatory and angiogenesis activity. On the other hand compound **10e**, which also comprises of the hydroxy group, but at para position of the phenyl ring attached to the 5th carbon atom of the oxadiazole ring showed IC₅₀ value as 250 µg/ml and this indicates that it has not shown remarkable activity.

2.2.3. Inhibition of inflammatory corneal neovascularization (CNV) by compound **10j**

The inflammatory corneal angiogenesis assay is one of the most reliable models to study the effect of drug on inflammatory angiogenesis, ever since the alkali burn creates the local inflammation in the cornea leading to the sprouting of new blood vessels. Three days after the corneal alkali burn, CNV occurred in both the control and treated groups (Fig. 1A). According to the results compared to the cornea of the control group, cornea in the compound **10j** treated group showed less CNV. The amount of CNV was quantified by measuring the area of neovascularization and it was found that the area of CNV was significantly smaller in the group treated with compound **10j** compared with the control group, which indicated an inhibitory effect of compound **10j** on CNV.

The haematoxylin and eosin (H and E) staining of the eyeball

Table 1

IC₅₀ values of compounds **10a-j** calculated based on HRBC membrane stabilization assay. Based on the IC₅₀ values, compounds **10j** was chosen as a lead compound.

Samples	HRBC membrane stabilization IC ₅₀ Value (µg/ml)
Control	–
10a	254
10b	273
10c	234
10d	239
10e	> 250
10f	194
10g	211
10h	> 250
10i	213
10j	153.43
Indomethacin	121.68

sections revealed that the primary infiltrating cells in the corneal stroma after the corneal alkali burn were inflammatory cells. The number of infiltrating cells in the corneal stroma were radically decreased in the compound **10j** treated group than in the control group. In the control group, the corneal epithelium was not repaired, the corneal stroma was thicker and more swollen than those in the compound **10j** treated group (Fig. 1B).

The chicken chorioallantoic membrane (CAM) assay was deployed to assess the inhibitory effect of compound **10j** on neovascularization, since it is considered as a more reliable model system to evaluate the angiopreventive and anti-inflammatory role of a test compound **10j** in *in-vivo* condition because this assay is a sensitive, inexpensive and easily feasible *in-vivo* model system to investigate potentially anti-inflammatory compounds [21]. In the present study rVEGF₁₆₅ induced neovascularisation in *in-vivo* CAM model was exposed with compound **10j**. A clear formation of a vascular zone around the implanted disc with compound **10j** as shown in the Fig. 1C and D was a clear evidence of the regression of neovessels in the developing embryos with compound **10j** which indicated the inhibition of angiogenesis.

2.2.4. Reduction of carrageenan induced paw oedema by compound **10j**

Carrageenan induced paw oedema is a well established animal model system to evaluate the anti-inflammatory drugs as it is acute, nonimmune, well researched and a highly reproducible model. The subcutaneous injection of carrageenan results in the release of pro-inflammatory agents and the inflammatory reaction is typically quantified by an increase in paw size (oedema).

Injection of mice with carrageenan caused a significant increase in the paw weight and percentage was measured after 5 h compared to the control values (Fig. 2A and B). Pretreatment of carrageenan injected mice with indomethacin 10 mg/kg body weight (*b.w*) significantly decreased paw volume to 40% and it was measured after 5 h compared to carrageenan injected mice. Whereas compound **10j** (25 mg/kg/*b.w*) treated animals revealed significantly decreased paw weight to 30% and it was measured after 5 h (75%) compared to that of carrageenan injected mice (Fig. 2).

2.2.5. MPO activity of compound **10j**

MPO corresponds to 1–5% of total protein in human neutrophils

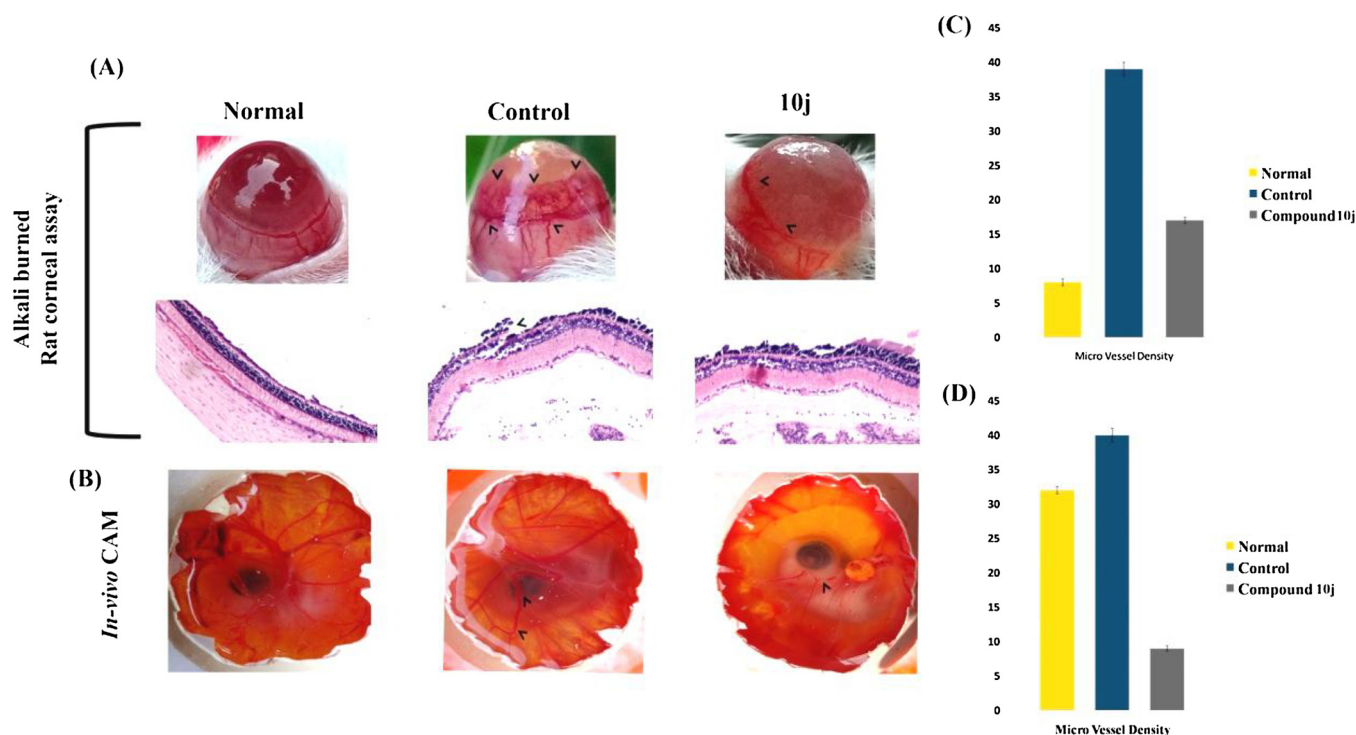


Fig. 1. Angiogenesis modulatory effect of compound 10j reduces the neovascularization. (A) Representative photographs of the rat cornea indicating the inhibition of angiogenesis in alkali burnt rat cornea and H and E staining of cornea showing improved corneal gesture with compound 10j treatment. (B) Decrease in total vessel length after compound 10j treatment in rat cornea. (C) *In vivo* CAM photos exhibits the angiopreventive effect of compound 10j. (D) Quantification of MVD of CAM.

[22,23]. The crux of the matter is that MPO was found at elevated levels within and near blood vessels in inflammatory conditions [24]. The neutrophil migration towards carrageenan induced inflammation in mouse paws was indirectly determined based on MPO activity in the target tissue. MPO secretion was a result of the host defense mechanism. Due to its importance during inflammatory processes and for being an indicator of the polymorphonuclear (PMN) presence in tissues, the MPO has been widely used as an inflammatory marker of both acute and chronic conditions. Positive control indomethacin treatment resulted in the decreased level of MPO activity. Treatment with compound 10j exhibited similar action in carrageenan induced paw oedema by significantly preventing the increase in MPO activity induced by carrageenan when compared to the control group (Fig. 2C).

2.2.6. Compound 10j inhibits COX-2 activity

Prostaglandins are lipid autacoids derived from arachidonic acid. They both maintain homeostatic regulation and also plays vital role in mediating pathogenic mechanisms, including the inflammatory response. The PG H2 synthase (cyclooxygenase or COX) is the crucial enzyme in the conversion of arachidonic acid to PGs. The PGs are prime mediators in physiological event, especially during inflammatory response [25]. COX-1 is consecutively expressed protein by most cell types and they are considered to take part in the PGs synthesis during physiological processes. Whereas COX-2 usually is absent, during normal physiological event, but is induced by numerous physiologic stimuli such as inflammation. Targeting the COX-2 expression level during inflammatory reaction will be a vital strategy. Following the promising potency of the compound 10j as anti-inflammatory agent, and COX-2 being the important factor in inflammatory reactions we first validated the effectiveness of the compound 10j under *in-vivo* approaches (Fig. 3E). On the other hand, by *in-silico* study the autodock programme was utilized to produce the protein-10j complex, in order to understand the interaction between COX-2 protein and compound 10j as shown in the Fig. 3A that ligand 10j is placed in the center of the active site and it is stabilized by hydrogen bonding interaction. The

hydrogen bond exhibited in the COX-2-10j complex have been documented, together with their distances and angles, by taking into account the interaction energies of the compound 10j with the active site of the COX-2 residue, a key active binding site of the model were determined and proved. Moreover, data revealed that the compound 10j formed hydrogen bonds with the amino acid ASP125, and an ionic interaction between carboxylic group of amino acid ALA86 and atom of oxadiazole ring of the compound 10j which contributed to the most stable binding of the S1 conformation from ligand to COX-2 with lowest binding energy at -7.11 kJ/mol (Fig. 3A–C). Further, the *in-silico* results were revalidated using *in-vivo* samples. By the mode of action of compound 10j the cellular COX-2 activity were measured in homogenate of paw tissue of the paw oedema animal experiment. The result inferred that compound 10j inhibited COX-2 activity by 26%, which is due to the presence of hydroxy substitution, particularly at the ortho position of the phenyl ring attached to the 5th carbon atom of the oxadiazole ring.

3. Conclusion

The present study has focused on the synthesis of a series of benzophenone integrated oxadiazoles (10a–j) with different substituents. Among the series 10a–j, compound 10j exhibited potential anti-inflammatory and anti-angiogenesis activity. The activity of synthesized compounds revealed that benzophenone appended oxadiazole plays a major role in enhancing the activity. From the study it is significant to note that the presence of hydroxy substituent, particularly at the ortho position of the phenyl ring attached to the 5th carbon atom of the oxadiazole ring exhibited a good anti-inflammatory and anti-angiogenesis activity. Among the series 10a–j, compound 10e has not shown remarkable activity, though it comprises the hydroxy group, but at para position of the phenyl ring attached to the 5th carbon atom of the oxadiazole ring.

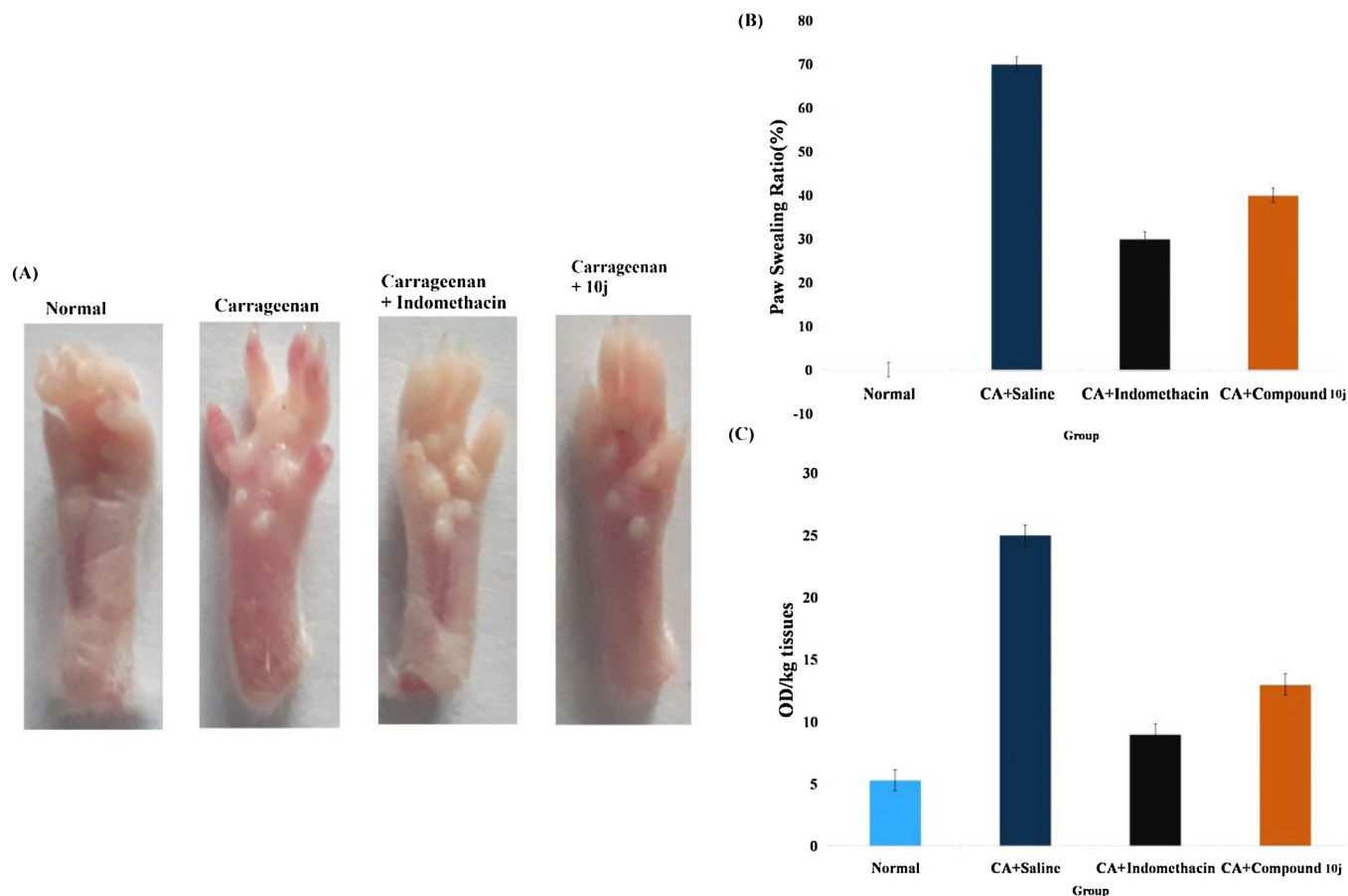


Fig. 2. Effect of compound 10j on carrageenan-induced paw oedema in mice. (A) Typical representative macroscopic photographs of paw from the normal, carrageenan + saline, carrageenan + indomethacin, carrageenan + compound 10j. (B) Paw swelling percentage after 48 h carrageenan injection in the different experimental animal. (C) Decreased MPO activity in compound 10j treated animal.

4. Materials and methods

4.1. Chemistry

Chemicals were purchased from Sigma Aldrich. Thin layer chromatography (TLC) was performed on aluminum backed silica plate which was visualized by UV-light. Melting points were determined on a Thomas Hoover capillary melting point apparatus with a digital thermometer. The IR spectra was recorded by the potassium bromide pellet method on FT-IR Shimadzu 8300 spectrophotometer, NMR spectra were recorded on a Bruker 400 MHz NMR spectrophotometer in DMSO and chemical shifts were recorded in parts per million down field from tetramethylsilane. Mass spectra were obtained with a VG70-70H spectrometer and elemental analysis results are within 0.4% of the calculated value.

4.1.1. General procedure for the preparation of methyl-4-hydroxybenzoate (2)

To the solution of 4-hydroxybenzoic acid (**1**, 0.028 mol) in methanol (25 ml), a catalytic amount of sulfuric acid was added and refluxed for 3 h, the reaction was monitored by TLC. After completion of the reaction, the organic layer was washed with sodium bicarbonate (3 × 15 ml), followed by distilled water (3 × 15 ml) and saturated sodium chloride solution (3 × 10 ml). The organic layer was dried over anhydrous sodium sulfate and the solvent was evaporated under reduced pressure to obtain compound **2**. The crude compound **2** was further purified by recrystallization with ethanol [26].

Yield: 83%; m.p: 124–126 °C; IR (KBr, γ/cm^{-1}): 1210 (C–O); 1672 (CO), 3312–3490 (OH), ^1H NMR (400 MHz, DMSO- d_6) δ : 3.8 (s, 3H,

CH_3), 5.8 (s, 1H, OH), 6.8–7.9 (m, 4H, ArH); ^{13}C NMR (100 MHz) δ : 52.21, 115.3, 121.82, 131.32, 160.34, 167.69; LCMS (M^+): (153); Anal.Calcd. for $\text{C}_8\text{H}_8\text{O}_3$: C, 63.15; H, 5.30; Found: C, 63.11; H, 5.36%.

4.1.2. General procedure for the preparation of methyl-4-(benzoyloxy) benzoate (3)

The mixture of compound (**2**, 0.016 mol), benzoyl chloride (0.016 mol) and TEA was stirred in a freezing mixture for 45 min and the reaction was monitored using TLC. After completion of the reaction, the organic layer was washed with sodium hydroxide, (3 × 10 ml) followed by distilled water (3 × 15 ml) and brine solution (3 × 10 ml). The organic solvent was dried over anhydrous sodium sulfate and the solvent was evaporated under reduced pressure to obtain compound (**3**) which was recrystallized from ethanol [27].

Yield: 71%; m.p: 98–101 °C; IR (KBr, γ/cm^{-1}): 1214 (C–O of OCOCH_3); 1315 (C–O of OCOPh), 1670 (C=O of OCOCH_3), 1725 (C=O of OCOPh), ^1H NMR (400 MHz, DMSO- d_6) δ : 3.4 (s, 3H, CH_3), 7.1–8.1 (m, 9H, ArH); ^{13}C NMR (100 MHz) δ : 51.11, 121.43, 127.54, 128.32, 130.12, 130.43, 130.56, 133.98, 134.81, 155.34, 165.21; LCMS (M^+): (257); Anal.Calcd. for $\text{C}_{15}\text{H}_{12}\text{O}_4$: C, 70.31; H, 4.72; Found: C, 70.37; H, 4.76%.

4.1.3. General procedure for the preparation of methyl-3-benzoyl-4-hydroxybenzoate (4)

Compound (**3**, 0.016 mol) and anhydrous aluminum chloride (0.032 mol) were heated to 120 °C for 20 min. Then cooled to room temperature and the complex was cleaved using 10% hydrochloric acid and the product was filtered, washed thoroughly with water (3 × 15 ml) and recrystallized with ethanol to afford compound **4** as a

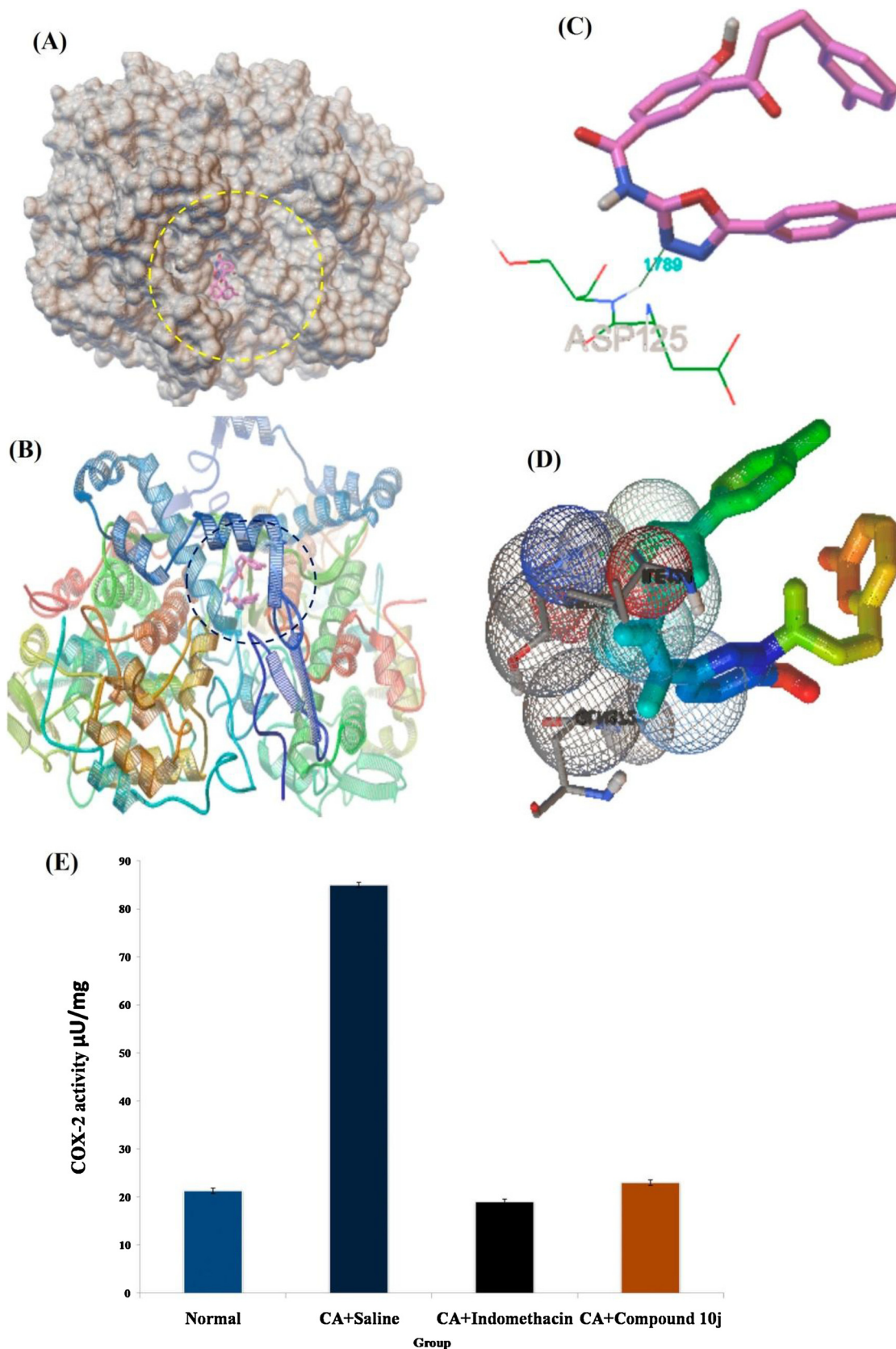


Fig. 3. Compound 10j interacts with COX-2 by binding with amino acid ASP125 through the hydrogen-bond. (A) 3D structure of the compound 10j in the active site C-terminal transactivation COX-2 complexes. (B) Ribbon models of COX-2 and the ligand molecule 10j complexes. (C) Hydrogen-bond interaction of the ligand molecule 10j with COX-2. (D) The 2D interactions analysis of 10j COX-2. (E) COX-2 activity in mice edematous tissue lysate treated with or without compound 10j.

pale yellow solid [28].

Yield: 83%; m.p 124–126 °C; IR (KBr, γ/cm^{-1}): 1232 (C–O of OCOCH₃), 1312 (C–O of COPh), 1676 (C=O of COPh), 1669 (C=O of OCOCH₃), 3328–3403 (OH); ¹H NMR (400 MHz, DMSO-*d*₆) δ : 2.9 (s, 3H, CH₃), 7.1–8.1 (m, 8H, ArH), 9.1 (s, 1H, OH); ¹³C-NMR (100 MHz) δ : 51.23, 115.21, 119.21, 122.65, 128.23, 130.43, 131.23, 132.65, 135.65, 139.21, 165.21, 166.23, 196.45; LCMS (M⁺): (257); Anal. Calcd. for C₁₅H₁₂O₄: C, 70.31; H, 4.72; Found: C, 70.23; H, 4.76%.

4.1.4. General procedure for the preparation of 3-benzoyl-4-hydroxybenzoic acid (5)

Compound (4, 0.016 mol) was refluxed with 20 ml of 10% sodium hydroxide in ethanol for 1 h and then acidified. A white solid separates out which was filtered and recrystallized with ethanol to achieve compound 5 [29].

Yield: 83%; m.p 138–140 °C; IR (KBr, γ/cm^{-1}): 1678 (C=O of COPh), 1716 (C=O of COOH), 3312–3355 (OH), 3450–3475 (OH of COOH); ¹H NMR (400 MHz, DMSO-*d*₆) δ : 6.8–7.9 (m, 8H, ArH), 11.2 (s, 1H, OH), 12.8 (s, 1H, COOH); ¹³C NMR (100 MHz) δ : 121.93, 125.43, 126.72, 130.24, 134.73, 137.06, 138.24, 139.43, 142.32, 165.65, 171.71, 201.52; LCMS (M⁺): (243); Anal. Calcd. for C₁₄H₁₀O₄: C, 69.42; H, 4.16; Found: C, 69.40; H, 4.09%.

4.1.5. General procedure for the preparation of 2-amino-5-phenyl-1,3,4-oxadiazole (9a)

A mixture of 1-benzylidenehydrazide (8a, 1.9 mmol) and CAT (2 mmol) in ethanol was refluxed with stirring for 3 h. The sodium chloride formed in the reaction was filtered off and washings were evaporated in vacuum and the residue was extracted with 10% hydrochloric acid (3 × 10 ml) and washed thoroughly with DCM. The aqueous layer was neutralized with 10% sodium hydroxide to achieve compound 9a, which was further purified by recrystallisation with methanol. The remaining compounds 9b–j were synthesized in the similar manner [18].

4.1.5.1. 2-Amino-5-phenyl-1,3,4-oxadiazole (9a). Yield: 81%; m.p: 240–242 °C; IR (KBr, γ/cm^{-1}): 1581 (C=N), 3475 (N–H of NH₂); ¹H NMR (400 MHz, DMSO-*d*₆) δ : 3.34 (s, 2H, NH₂), 7.13–7.65 (m, 5H, ArH); ¹³C NMR (100 MHz) δ : 124.23, 125.02, 127.32, 128.41, 157.11, 164.32; LCMS (M⁺): (162); Anal. Calcd. for C₈H₇N₃O: C, 59.62; H, 4.38; N, 26.07; Found: C, 59.64; H, 4.36; N, 26.08%.

4.1.5.2. 2-Amino-5-(4-bromo)phenyl-1,3,4-oxadiazole (9b). Yield: 85%; m.p: 223–226 °C; IR (KBr, γ/cm^{-1}): 1579 (C=N), 3472 (N–H of NH₂); ¹H NMR (400 MHz, DMSO-*d*₆) δ : 3.31 (s, 2H, NH₂), 7.13–7.65 (m, 4H, ArH), ¹³C NMR (100 MHz) δ : 123.23, 125.42, 129.32, 132.41, 156.91, 163.32; LCMS (M⁺): (239) Anal. Calcd. for C₈H₆BrN₃O: C, 40.03; H, 2.52; N, 17.50; Found: C, 40.24; H, 2.52; N, 17.58%.

4.1.5.3. 2-Amino-5-(3-methoxy)phenyl-1, 3, 4-oxadiazole (9c). Yield: 83%; m.p: 181–183 °C; IR (KBr, γ/cm^{-1}): 3432 (N–H of NH₂), 1564 (C=N); ¹H NMR (400 MHz, DMSO-*d*₆) δ : 3.32 (s, 3H, OCH₃), 3.31 (s, 2H, NH₂), 7.13–7.65 (m, 4H, ArH), ¹³C NMR (100 MHz) δ : 164.65, 161.32, 156.54, 130.41, 127.32, 114.32, 119.65, 111.43, 55.23; LCMS (M⁺): (191); Anal. Calcd. for C₉H₉N₃O₂: C, 56.54; H, 4.74; N, 21.98; Found: C, 56.52; H, 4.72; N, 21.68%.

4.1.5.4. 2-Amino-5-(2,6-dimethoxy)phenyl-1,3,4-oxadiazole (9d). Yield: 74%; m.p: 154–157 °C; IR (KBr, γ/cm^{-1}): 3443 (N–H of NH₂), 1552 (C=N); ¹H NMR (400 MHz, DMSO-*d*₆) δ : 3.36 (s, 6H, OCH₃), 3.39 (s, 2H, NH₂), 7.13–7.65 (m, 3H, ArH), ¹³C NMR (100 MHz) δ : 165.32, 157.42, 153.17, 148.34, 113.45, 115.92, 115.12, 111.43, 57.23; LCMS (M⁺): (222); Anal. Calcd. For C₁₀H₁₁N₃O₃: C, 54.29; H, 5.01; N, 19.00; Found: C, 54.22; H, 5.06; N, 19.08%.

4.1.5.5. 2-Amino-5-(4-hydroxy)phenyl-1,3,4-oxadiazole (9e). Yield:

89%, m.p 150–153 °C; IR (KBr, γ/cm^{-1}): 1549 (C=N), 3343–3365 (OH), 3454 (N–H of NH₂); ¹H NMR (400 MHz, DMSO-*d*₆) δ : 3.39 (s, 2H, NH₂), 7.13–7.65 (m, 4H, ArH), 9.1 (s, 1H, OH); ¹³C NMR (100 MHz) δ : 116.92, 118.45, 129.91, 157.22, 159.19, 164.32; LCMS (M⁺): (178); Anal. Calcd. for C₈H₇N₃O₂: C, 54.24; H, 3.98; N, 23.72; Found: C, 54.24; H, 3.96; N, 23.81%.

4.1.5.6. 2-Amino-5-(2,4-dimethoxy)phenyl-1,3,4-oxadiazole (9f). Yield: 83%; m.p: 163–166 °C; IR (KBr, γ/cm^{-1}): 1543 (C=N), 3441 (N–H of NH₂); ¹H NMR (400 MHz, DMSO-*d*₆) δ : 3.21 (s, 6H, OCH₃), 3.31 (s, 2H, NH₂), 7.13–7.65 (m, 3H, ArH), ¹³C NMR (100 MHz) δ : 56.2, 101.23, 106.12, 130.23, 157.32, 161.37, 164.12; LCMS (M⁺): (222) Anal. Calcd. for C₁₀H₁₁N₃O₃: C, 54.29; H, 5.01; N, 19.00; Found: C, 54.28; H, 5.04; N, 19.03%.

4.1.5.7. 2-Amino-5-(4-chloro)phenyl-1,3,4-oxadiazole (9g). Yield: 79%; m.p: 210–213 °C; IR (KBr, γ/cm^{-1}): 1584 (C=N), 3469 (N–H of NH₂); ¹H NMR (400 MHz, DMSO-*d*₆) δ : 3.30 (s, 2H, NH₂), 7.13–7.65 (m, 4H, ArH); ¹³C NMR (100 MHz) δ : 123.43, 127.32, 129.23, 136.23, 156.43, 163.21; LCMS (M⁺): (196) (198); Anal. Calcd. for C₈H₆ClN₃O: C, 49.12; H, 3.09; N, 21.48; Found: C, 49.14; H, 3.06; N, 21.48%.

4.1.5.8. 2-Amino-5-(3-bromo)phenyl-1,3,4-oxadiazole (9h). Yield: 83%; m.p: 146–148 °C; IR (KBr, γ/cm^{-1}): 1568 (C=N), 3476 (N–H of NH₂); ¹H NMR (400 MHz, DMSO-*d*₆) δ : 3.29 (s, 2H, NH₂), 7.13–7.65 (m, 4H, ArH), ¹³C NMR (100 MHz) δ : 124.21, 128.32, 129.23, 126.23, 131.21, 133.61, 156.65, 165.21; LCMS (M⁺): (239); Anal. Calcd. For C₈H₆BrN₃O: C, 40.03; H, 2.52; N, 17.50; Found: C, 40.04; H, 2.54; N, 17.53%.

4.1.5.9. 2-Amino-5-(2-methoxy)phenyl-1,3,4-oxadiazole (9i). Yield: 70%; m.p: 132–135 °C; IR (KBr, γ/cm^{-1}): 1551 (C=N), 3442 (N–H of NH₂); ¹H NMR (400 MHz, DMSO-*d*₆) δ : 3.28 (s, 3H, OCH₃), 3.43 (s, 2H, NH₂), 7.13–7.65 (m, 4H, ArH), ¹³C NMR (100 MHz) δ : 57.2, 110.21, 115.23, 120.32, 122.34, 128.32, 156.21, 157.12, 166.32; LCMS (M⁺): (191); Anal. Calcd. for C₉H₉N₃O₂: C, 56.54; H, 4.74; N, 21.98; Found: C, 56.56; H, 4.76; N, 21.93%.

4.1.5.10. 2-Amino-5-(2-hydroxy)phenyl-1,3,4-oxadiazole (9j). Yield: 81%, m.p: 123–126 °C; IR (KBr, γ/cm^{-1}): 1530 (C=N), 3329–3345 (OH), 3464 (N–H of NH₂); ¹H NMR (400 MHz, DMSO-*d*₆) δ : 3.21 (s, 2H, NH₂), 7.13–7.65 (m, 4H, ArH), 9.6 (s, 1H, OH); ¹³C NMR (100 MHz) δ : 113.21, 117.21, 126.02, 128.05, 130.91, 155.22, 156.29, 163.12; LCMS (M⁺): (178); Anal. Calcd. For C₈H₇N₃O₂: C, 54.24; H, 3.98; N, 23.72; Found: C, 54.14; H, 3.95; N, 23.83%.

4.1.6. General procedure for the preparation of 2(4-hydroxy)-3-benzoyl benzamide-5-(phenyl) 1,3,4 oxadiazole (10a)

To the stirring solution of compound (5, 1.9 mmol) in 10 ml of DMSO, TEA was added, followed by the addition of coupling agent HATU (2.0 mmol). The mixture was stirred for 20 min at room temperature, to this stirring solution compound 9a was added and the stirring was continued. Further, the reaction was monitored by TLC, after completion of the reaction, the reaction mass was treated with ethyl acetate and the organic layer was washed with 10% sodium bicarbonate solution (3 × 15 ml) followed by 10% hydrochloric acid (3 × 15 ml). Finally the mixture was washed with water (3 × 15 ml), then the organic layer was evaporated under reduced pressure to achieve title compound 10a. The crude compound was recrystallized with ethanol and the remaining compounds 10b–j were synthesized in the similar manner [19].

4.1.6.1. 2(4-Hydroxy-3-benzoyl) benzamide-5-(phenyl) 1,3,4-oxadiazole (10a). Yield: 83%, m.p: 161–163 °C; IR (KBr, γ/cm^{-1}): 1580 (C=N), 1679 (C=O of COPh), 1680 (C=O of CONH), 3310–3385 (OH), 3600 (NH of CONH), ¹H NMR (400 MHz, DMSO-*d*₆) δ : 7.1–8.1 (m, 13H, ArH),

8.1 (s, 1H, CONH), 9.5 (s, 1H, OH); ^{13}C NMR (100 MHz) δ : 119.56, 114.65, 126.12, 126.34, 126.76, 128.42, 128.94, 129.12, 129.54, 130.61, 132.64, 133.03, 139.72, 157.65, 163.23, 163.75, 164.22, 196.43; LCMS (M^+): (386); Anal. Calcd. for $\text{C}_{22}\text{H}_{15}\text{N}_3\text{O}_4$: C, 68.57; H, 3.92; N, 10.90; Found: C, 68.54; H, 3.94; N, 10.93%.

4.1.6.2. *2(4-Hydroxy-3-benzoyl) benzamide-5-(4-bromophenyl) 1,3,4-oxadiazole (10b)*. Yield: 69%; m.p:145–148 °C; IR (KBr, γ/cm^{-1}): 1584 (C=N), 1675 (C=O of COPh), 1683 (C=O of CONH), 3345–3395 (OH), 3599 (NH of CONH); ^1H NMR (400 MHz, DMSO- d_6) δ : 7.1–8.1 (m, 12H, ArH), 8.3 (s, 1H, CONH), 9.7 (s, 1H, OH); ^{13}C NMR (100 MHz) δ : 116.01, 118.16, 123.52, 125.34, 126.66, 128.34, 129.12, 129.53, 130.31, 131.89, 132.23, 132.64, 138.62, 157.45, 164.25, 164.75, 165.23, 196.53; LCMS (M^+): (465) Anal. Calcd. for $\text{C}_{22}\text{H}_{14}\text{BrN}_3\text{O}_4$: C, 56.91; H, 3.04; N, 9.05; Found: C, 56.94; H, 3.06; N, 9.09%.

4.1.6.3. *2(4-Hydroxy-3-benzoyl) benzamide-5-(3-methoxyphenyl)1,3,4-oxadiazole (10c)*. Yield: 81%; m.p: 135–138 °C; IR (KBr, γ/cm^{-1}): 1582 (C=N), 1675 (C=O of COPh), 1684 (C=O of CONH), 3339–3374 (OH), 3586 (NH of CONH); ^1H NMR (400 MHz, DMSO- d_6) δ : 3.61 (s, 3H, OCH₃) 7.1–8.1 (m, 12H, ArH), 8.6 (s, 1H, CONH), 9.4 (s, 1H, OH); ^{13}C NMR (100 MHz) δ : 57.6, 111.23, 114.31, 115.16, 119.12, 119.34, 126.56, 127.43, 128.34, 129.12, 130.21, 130.41, 132.53, 132.72, 138.12, 157.29, 161.34, 164.31, 164.72, 165.43, 196.51; LCMS (M^+): (416); Anal. Calcd. for $\text{C}_{23}\text{H}_{17}\text{N}_3\text{O}_5$: C, 66.50; H, 4.12; N, 10.12; Found: C, 66.54; H, 4.16; N, 10.12%.

4.1.6.4. *2(4-Hydroxy-3-benzoyl) benzamide-5-(2, 6 dimethoxyphenyl) 1,3,4-oxadiazole (10d)*. Yield: 78%; m.p: 135–138 °C; IR (KBr, γ/cm^{-1}): 1588 (C=N), 1677 (C=O of COPh), 1685 (C=O of CONH), 3347–3356 (OH), 3580 (NH of CONH); ^1H NMR (400 MHz, DMSO- d_6) δ : 3.21(s, 6H, OCH₃) 7.1–8.1 (m, 11H, ArH), 8.3 (s, 1H, CONH), 9.7 (s, 1H, OH); ^{13}C NMR (100 MHz) δ : 56.6, 111.32, 112.23, 116.01, 118.16, 123.52, 126.66, 128.34, 129.53, 129.12, 130.31, 132.23, 132.64, 138.62, 157.45, 164.25, 164.75, 165.23, 196.53; LCMS (M^+): (467); Anal. Calcd. For $\text{C}_{24}\text{H}_{19}\text{N}_3\text{O}_6$: C, 64.72; H, 4.30; N, 9.43; Found: C, 64.54; H, 4.29; N, 9.42%.

4.1.6.5. *2(4-Hydroxy-3-benzoyl) benzamide-5-(4-hydroxyphenyl) 1,3,4-oxadiazole (10e)*. Yield: 87%; m.p: 143–145 °C; IR (KBr, γ/cm^{-1}): 1576 (C=N), 1672 (C=O of COPh), 1679 (C=O of CONH), 3334–3356 (OH), 3586 (NH of CONH); ^1H NMR (400 MHz, DMSO- d_6) δ : 7.1–8.1 (m, 12H, ArH), 8.3 (s, 1H, CONH), 9.2 (s, 1H, OH), 9.7 (s, 1H, OH); ^{13}C NMR (100 MHz) δ : 115.32, 116.01, 116.23, 118.16, 119.34, 126.76, 128.53, 128.84, 130.61, 132.23, 133.64, 139.02, 157.43, 158.43, 164.82, 164.81, 165.53, 196.26; LCMS (M^+): (402); Anal. Calcd. for $\text{C}_{22}\text{H}_{15}\text{N}_3\text{O}_5$: C, 65.83; H, 3.77; N, 10.47; Found: C, 65.84; H, 3.79; N, 10.42%.

4.1.6.6. *2(4-Hydroxy-3-benzoyl) benzamide-5-(1, 3 dimethoxyphenyl) 1,3,4-oxadiazole (10f)*. Yield: 81%; m.p: 167–170 °C; IR (KBr, γ/cm^{-1}): 1587 (C=N), 1671 (C=O of COPh), 1679 (C=O of CONH), 3343–3365 (OH), 3589 (NH of CONH); ^1H NMR (400 MHz, DMSO- d_6) δ : 3.21(s, 6H, OCH₃) 7.1–8.1 (m, 11H, ArH), 8.3 (s, 1H, CONH), 9.1 (s, 1H, OH) ^{13}C NMR (100 MHz) δ : 56.32, 57.6, 100.23, 102.31, 106.36, 115.12, 119.74, 126.13, 128.44, 129.32, 129.61, 130.71, 132.43, 132.92, 138.42, 157.69, 158.45, 161.67, 164.31, 164.92, 165.73, 196.63; LCMS (M^+): (446); Anal. Calcd. for $\text{C}_{24}\text{H}_{19}\text{N}_3\text{O}_6$: C, 64.72; H, 4.30; N, 9.43; Found: C, 64.74; H, 4.36; N, 9.42%.

4.1.6.7. *2(4-Hydroxy-3-benzoyl) benzamide-5-(4 chlorophenyl) 1,3,4-oxadiazole (10g)*. Yield: 85%; m.p: 205–208 °C; IR (KBr, γ/cm^{-1}): 1578 (C=N), 1679 (C=O of COPh), 1686 (C=O of CONH), 3341–3375 (OH), 3576 (NH of CONH); ^1H NMR (400 MHz, DMSO- d_6): δ 7.1–8.1 (m, 12H, ArH), 8.8 (s, 1H, CONH), 9.6 (s, 1H, OH); ^{13}C

NMR (100 MHz) δ : 115.01, 119.16, 124.24, 125.23, 126.16, 128.54, 129.23, 129.62, 130.01, 132.43, 132.43, 134.64, 139.52, 157.45, 165.25, 164.55, 164.93, 196.73; LCMS (M^+): (419); Anal. Calcd. For $\text{C}_{22}\text{H}_{14}\text{ClN}_3\text{O}_4$: C, 62.94; H, 3.36; N, 10.01; Found: C, 62.94; H, 3.06; N, 10.09%.

4.1.6.8. *2(4-Hydroxy-3-benzoyl) benzamide-5-(3-bromophenyl) 1,3,4-oxadiazole (10h)*. Yield: 79%; m.p:165–168 °C; IR (KBr, γ/cm^{-1}): 1583 (C=N), 1674 (C=O of COPh), 1686 (C=O of CONH), 3349–3386 (OH), 3587 (NH of CONH); ^1H NMR (400 MHz, DMSO- d_6) δ : 7.1–8.1 (m, 12H, ArH), 8.3 (s, 1H, CONH), 9.7 (s, 1H, OH); ^{13}C NMR (100 MHz) δ : 115.71, 119.32, 123.21, 126.44, 126.65, 128.23, 128.45, 129.32, 129.43, 130.42, 131.56, 131.78, 132.46, 132.33, 133.54, 139.62, 156.95, 164.44, 164.66, 165.53, 196.43; LCMS (M^+): (465); Anal. Calcd. for $\text{C}_{22}\text{H}_{14}\text{BrN}_3\text{O}_4$: C, 56.91; H, 3.04; N, 9.05; Found: C, 56.98; H, 3.05; N, 9.06%.

4.1.6.9. *2(4-Hydroxy-3-benzoyl) benzamide-5-(2-methoxyphenyl) 1,3,4-oxadiazole (10i)*. Yield: 91%; m.p:143–146 °C; IR (KBr, γ/cm^{-1}): 1584 (C=N), 1676 (C=O of COPh), 1682 (C=O of CONH), 3345–3376 (OH), 3576 (NH of CONH); ^1H NMR (400 MHz, DMSO- d_6): δ 3.54 (s, 3H, OCH₃) 7.1–8.1 (m, 12H, ArH), 8.4 (s, 1H, CONH), 9.6 (s, 1H, OH); ^{13}C NMR (100 MHz) δ : 57.6, 110.51, 115.46, 114.82, 119.64, 121.36, 126.23, 128.34, 129.45, 129.12, 130.43, 132.56, 132.52, 135.23, 139.52, 158.75, 157.59, 164.31, 164.54, 165.45, 196.23; LCMS (M^+): (416); Anal. Calcd. for $\text{C}_{23}\text{H}_{17}\text{N}_3\text{O}_5$: C, 66.50; H, 4.12; N, 10.12; Found: C, 66.53; H, 4.12; N, 10.13%.

4.1.6.10. *2(4-Hydroxy-3-benzoyl) benzamide-5-(2-hydroxyphenyl) 1,3,4-oxadiazole (10j)*. Yield: 78%; m.p:130–133 °C; IR (KBr, γ/cm^{-1}): 1572 (C=N), 1669 (C=O of CONH), 1678 (C=O of COPh), 3335–3365 (OH), 3582 (NH of CONH); ^1H NMR (400 MHz, DMSO- d_6) δ : 7.1–8.1 (m, 12H, ArH), 8.5 (s, 1H, CONH), 9.4 (s, 1H, OH) 9.8 (s, 1H, OH) ^{13}C NMR (100 MHz) δ : 115.71, 119.66, 123.64, 126.55, 126.83, 128.54, 128.43, 129.52, 130.31, 131.31, 132.23, 132.63, 133.33, 139.42, 157.43, 164.41, 164.82, 165.64, 196.28; LCMS (M^+): (402); Anal. Calcd. for $\text{C}_{22}\text{H}_{15}\text{N}_3\text{O}_5$: C, 65.83; H, 3.77; N, 10.47; Found: C, 65.79; H, 3.73; N, 10.48%.

4.2. Biology

4.2.1. HRBC membrane stabilization assay

The HRBC membrane stabilization has been used as a method to investigate the anti-inflammatory activity. Series of compounds **10a–j** were used for the *in vitro* anti-inflammatory activity [30]. In brief, blood was collected from healthy human volunteer who had not taken any non-steroidal anti-inflammatory drugs (NSAIDS) for two weeks prior to the experiment and mixed with equal volume of sterilized alsever's solution (2% dextrose, 0.8% sodium citrate, 0.5% citric acid and 0.55% sodium chloride). The blood was centrifuged at 3000 revolutions per minute (rpm) and packed cells were washed with isosaline (0.9% w/v sodium chloride) and a 10% suspension of blood was made with isosaline. Various concentrations of the compounds **10a–j** were prepared (0, 50, 100, 150, 200 and 250 $\mu\text{g}/\text{ml}$) using DMSO and to each concentration 1 ml phosphate buffer, 2 ml hyposaline, and 0.5 ml HRBC suspension were added. Then the mixture was incubated at 37 °C for 30 min and centrifuged at 3000 rpm for 20 min and the hemoglobin content in the supernatant solution was estimated spectrophotometrically at 560 nm. Indomethacin (50, 100, 150, 200 and 250 $\mu\text{g}/\text{ml}$) was used as a reference and a control was prepared without the compounds **10a–j**. The hemolysis percentage was calculated by assuming the hemolysis produced by the control group as 100%. The percentage of HRBC membrane stabilization or protection was calculated using the formula, percent protection = $100 - (\text{OD of compound treated sample} / \text{OD of control} \times 100)$.

4.2.2. *In vivo* CAM assay

The *in vivo* CAM assay was performed according to the standard protocol [8]. In brief, fertilized hen's eggs were procured from Indian Veterinary Institute Poultry Department, Bengaluru. All the eggs were incubated at 37 °C in a humidified incubator (Rotex, India). On the 11th day of incubation, all the eggs were grouped separately with each group containing minimum six eggs. Group A served as normal with no treatment, group B served as control group treated with rVEGF165 (1 µg) (Produced in Molecular Biomedicine laboratory, Department of Biotechnology, Sahyadri Science College, Shivammogga alone) and group C served as a test group, treated with compound **10j** (5 µM) + rVEGF165 (1 µg). The windows were opened after 48 h *i.e.* on the 13th day of incubation, inspected and quantified for changes in the MVD and photographed using Sony steady shot DSC-W610 camera.

4.2.3. Animals and ethics

The animal models used for the study include healthy Swiss albino male mice weighing 25 ± 2.0 g and Swiss albino male rat weighing 150 ± 5.0 g. All the animals were grouped separately and housed in polyacrylic cages and maintained under standard conditions (25 ± 2 °C). All procedures described were reviewed and approved by the National College of Pharmacy Ethical Committee, Shivammogga, India, in accordance with the CPCSEA guidelines for laboratory animal facility (NCP/IAEC/CL/101/05/ 2012-13).

4.2.4. Determination of the lethal dose 50 (LD50) of the compounds **10a–j**

For the determination of LD50 of the series of compounds **10a–j**, 'staircase' method [10] was employed. Healthy Swiss albino male mice weighing 25 ± 5 g were used and were divided into 12 groups of six animals in each group for all the compounds. The test compounds **10a–j** were dissolved in DMSO and administered *i.p.*, in increasing levels of 100, 200, 300, 400, and 500 mg/kg body weight of the animals. The animals were then observed continuously for 3 h for general behavioral, neurological, and autonomic profiles and then every 30 min for the next 3 h and finally the animals were died after 24 h. The maximum non lethal and the minimum lethal doses were thus determined. One tenth and one twentieth of this LD₅₀ dose was selected as the therapeutic dose for the evaluation of *in vivo* anti-angiogenic activity of the compounds **10a–j**.

4.2.5. Induction of alkali burn-induced corneal neovascularization

Corneal neovascularization was induced by alkali injury, as reported earlier with little modification [31]. The Swiss albino Wistar rats were examined and found to have no ophthalmic diseases before alkali burn. Animals were divided into three groups and each group consists of 6 animals (n = 6). Group A: normal animal without any treatment, animals from group B were treated as control animals and the group C animals served as a **10j** treated group.

Corneal alkali burn was generated in the right eye of animals from group B and group C after general anesthesia by a combined intraperitoneal injection of katamine (1 ml/kg) and chlorpromazine (1 ml/kg). A piece of Whatman filter paper (3-mm diameter) soaked in 4 ml sodium hydroxide (1 mol/l) was applied to the center of the cornea for 40 s. The alkali treated cornea was then irrigated with 60 ml of normal saline. The area of corneal neovascularization was quantified by photographic documentation after 48 h of alkali burn. Animals from group C were used to treat the alkali burnt cornea by compound **10j** (5 µg). Neovascular inhibitory effect of compound **10j** was assessed by photographic documentation after 24 h of compound **10j** treatment.

4.2.6. Carrageenan-induced paw oedema in mice

Male Swiss albino mice were selected for the study of anti-inflammatory effect of compound **10j** against carrageenan induced paw oedema [32]. For this study, experimental animals were divided into four groups, each group consists of six animals (n = 6). Group I animals are served as normal animals with no treatment. Prior to experiment

animals from group II were injected with saline (5 ml/kg), group III animals were injected with positive control (10 mg/kg/b.w), group IV animals were injected with a test compound **10j** (25 mg/kg/b.w) and animals were left in a respective cage for 2 h. After 2 h animals from the control, positive control, and test group were injected with 100 µl of 2% carrageenan at the right paw. The right paw of all the experimental animals was observed with different time intervals (2 h, 3 h and 5 h) and volume of the paw was measured using digital plethysmometer. After 24 h the right hind paw tissue was rinsed in ice-cold normal saline, and immediately placed in its four volumes of cold normal saline and homogenized at 4 °C. Then the homogenate was centrifuged at 12,000 rpm for 5 min. Then the supernatant was stored at –80 °C for the COX-2, activity assays.

4.2.7. MPO assays

The tissue MPO activity of compound **10j**, using a standard protocol method with little modification was performed [33]. The tissue from the carrageenan induced paw oedema experimental mice were used to assess the MPO activity, after the 4 h carrageenan administration. The tissue samples from all groups of animals were placed in 0.75 ml of 80 mM phosphate buffered saline, pH 5.4, containing 0.5% hexadecyltrimethylammonium bromide (HTAB), and were then homogenized 45 s at 0 °C in a homogenizer. The homogenate was decanted into a microfuge tube and the vessel was washed with a second 0.75 ml aliquot of HTAB in the buffer. The washing was transferred to a microfuge tube, and centrifuged at 12,000 rpm at 4 °C for 15 min. About 30 µl resulted supernatant solution were added to 96-well microtitre plates, then 200 µl of a mixture containing phosphate buffered saline (100 µl, 80 mM), pH 5.4, phosphate buffered saline (85 µl, 0.22 mM), pH 5.4, and hydrogen peroxide (15 µl–0.017%) was added to the wells. The reaction was initiated by the addition of tetramethyl benzidine-hydrochloride (20 µl, 18.4 mM) in dimethylformamide. Then the plates were incubated at 37 °C for 3 min and the reaction was stopped by the addition of sodium acetate (30 µl of 1.46 M) pH 3.0. Finally, the enzyme activity was determined calorimetrically using a plate reader, at 630 nm and expressed as MOD/mg tissue.

4.2.8. COX-2 activity assay

The COX-2 activity was measured in mice edematous tissue lysate treated with or without compound **10j** in accordance with the previously described methods with slight modifications [34]. Briefly, after 24 h post treatment paws were homogenized in RIPA buffer and protein concentration was determined. COX enzymatic activity was determined with 100 mg of protein in 0.2 ml volume of assay buffer (100 mM tris-hydrochloride pH 7.8, 5 mM tryptophan, and 5 mM reduced glutathione). Samples were incubated at 37 °C for 15 min in the presence of an excess arachidonic acid (100 mM). The reaction was stopped by boiling, and samples were centrifuged at 10,000 rpm for 10 min. Concentrations of PGs were measured according to the manufacturer's instructions (Cayman Chemical).

4.2.9. *In-silico* studies

Molecular modeling investigations were carried out using autodock tools-1.5.6.4 GB RAM, 5000 GB hard disk, and NVIDIA Quadro FX 4500 graphics card which was employed in the docking studies. The compounds used for docking was converted into 3D with ChemBio3D Ultra 14.0. The mouse COX-2 (4rry model) taken as a model for the human COX-2 enzyme which was obtained from protein data bank (PDB 4rry). Using tools available in autodock programmer the proteins and ligands were downloaded and prepared in three-dimensional atomic coordinates for molecular docking. All molecular modeling experiments were carried out with cartoon and ribbon models and the Figures showing protein-ligand interactions were generated using PyMOL.

Conflict of interest statement

The authors hereby state that they have no conflict of interest.

Acknowledgements

Naveen P. gratefully acknowledges the financial support of UGCMRP(S)-0551-13-14/KAMY013/UGC-SWRO. S. A. Khanum greatly acknowledges the financial support provided by the Vision Group on Science and Technology, Bangalore, Government of Karnataka, under the scheme CISEE (VGST/CISEE/2012-13/282), India. B.T. Prabhakar and Vikas H.M. gratefully acknowledges for the grant support by VGST (VGST/P-2/CISEE/GRD-231/2013-14). Also the authors are thankful to the Principals, JSS College of Arts, Commerce and Science, Mysuru Yuvaraja's College, Mysuru and Sahyadri Science College (Autonomous), Kuvempu University, Shivammogga for providing laboratory facilities.

References

- [1] R. Chovatiya, R. Medzhitov, Stress, inflammation, and defense of homeostasis, *Mol. Cell* 54 (2014) 281–288.
- [2] C. Costa, J. Incio, R. Soares, Angiogenesis and chronic inflammation cause or consequence, *Angiogenesis* 10 (2007) 149–166.
- [3] E.L. Assar, M.J. Angulo, L. Rodríguez-Manas, Oxidative stress and vascular inflammation in aging, *Free Radic. Biol. Med.* 65 (2013) 380–401.
- [4] J. Olza, C.M. Aguilera, M. Gil-Campos, R. Leis, G. Bueno, M.D. Martínez-Jiménez, M. Valle, R. Canete, R. Tojo, L.A. Moreno, A. Gil, Myeloperoxidase is an early biomarker of inflammation and cardiovascular risk in prepubertal obese children, *Diabetes Care* 35 (2012) 2373–2386.
- [5] B.D. Lowe, W.J. Storkus, Chronic inflammation and immunologic-based constraints in malignant disease, *Immunotherapy* 10 (2011) 1265–1274.
- [6] E.R. Rayburn, S.J. Ezell, R. Zhang, Anti-inflammatory agents for cancer therapy, *Mol. Cell Pharmacol.* 11 (2009) 29–43.
- [7] Y.H.E. Mohammed, V.H. Malojirao, P. Thirusangu, M. Al-Ghorbani, B.T. Prabhakar, S.A. Khanum, The novel 4-phenyl-2-phenoxyacetamide thiazoles modulates the tumor hypoxia leading to the crackdown of neoangiogenesis and evoking the cell death, *Eur. J. Med. Chem.* 143 (2018) 1826–1839.
- [8] Y.H.E. Mohammed, P. Thirusangu, Zabiulla, B.T. Prabhakar, S.A. Khanum, The anti-invasive role of novel synthesized pyridazine hydrazide appended phenoxy acetic acid against neoplastic development targeting matrix metallo proteases, *Biomed. Pharmacother.* 95 (2017) 375–386.
- [9] Zabiulla, H.G. Shamanth Neralagundi, A. Bushra Begum, B.T. Prabhakar, S.A. Khanum, Design and synthesis of diamide-coupled benzophenones as potential anticancer agents, *Eur. J. Med. Chem.* 115 (2016) 342–351.
- [10] H.D. Gurupadaswamy, P. Thirusangu, B.R. Vijay Avin, V. Vigneshwaran, M.V. Prashanth Kumar, T.S. Abhishek, V. Lakshmi Ranganatha, S.A. Khanum, B.T. Prabhakar, DAO-9(2,5-di(4-aryloylaryloxymethyl)-1,3,4-oxadiazole) exhibits p53 induced apoptosis through caspase-3 mediated endonuclease activity in murine carcinoma, *Biomed. Pharmacother.* 13 (2014) 791–799.
- [11] M.S. Madhu, U. Nagarjuna, V. Padmavathi, A. Padmaja, N.V. Reddy, T. Vijaya, Synthesis and antimicrobial activity of pyrimidinyl 1,3,4-oxadiazoles, 1,3,4-thiadiazoles and 1,2,4-triazoles, *Eur. J. Med. Chem.* 145 (2018) 11–21.
- [12] E. Durgashivaprasad, G. Mathew, S. Sebastian, S.A. Reddy, J. Mudgal, G.K. Nampurath, Novel 2,5-disubstituted-1,3,4-oxadiazoles as anti-inflammatory drugs, *Indian J. Pharmacol.* 46 (2014) 521–630.
- [13] S. Bansal, M. Bala, S.K. Suthar, S. Choudhary, S. Bhattacharya, V. Bhardwaj, S. Singla, A. Joseph, Design and synthesis of novel 2-phenyl-5-(1,3-diphenyl-1H-pyrazol-4-yl)-1,3,4-oxadiazoles as selective COX-2 inhibitors with potent anti-inflammatory activity, *Eur. J. Med. Chem.* 80 (2014) 167–174.
- [14] P. Singh, P.K. Sharma, J.K. Sharma, A. Upadhyay, N. Kumar, Synthesis and evaluation of substituted diphenyl-1,3,4-oxadiazole derivatives for central nervous system depressant activity, *Org. Med. Chem. Lett.* 2 (2012) 28–36.
- [15] R. Khanam, K. Ahmad, I.I. Hejazi, I.A. Siddique, V. Kumar, A.R. Bhat, A. Azam, F. Athar, Inhibitory growth evaluation and apoptosis induction in MCF-7 cancer cells by new 5-aryl-2-butylthio-1,3,4-oxadiazole derivatives, *Cancer Chemother. Pharmacol.* 80 (2017) 1027–1042.
- [16] A. Kumar, S.S. D'Souza, S.R. Nagaraj, S.L. Gaonkar, B.P. Salimath, K.M. Rai, Antiangiogenic and antiproliferative effects of substituted-1,3,4-oxadiazole derivatives is mediated by down regulation of VEGF and inhibition of translocation of HIF-1alpha in Ehrlich ascites tumor cells, *Cancer Chemother. Pharmacol.* 64 (2009) 1221–1233.
- [17] A. Kamal, P.S. Srikanth, M.V. Vishnuvardhan, G.B. Kumar, K.S. Babu, S.M. Hussaini, J.S. Kapure, A. Alarifi, Combretastatin linked 1,3,4-oxadiazole conjugates as a Potent Tubulin Polymerization inhibitors, *Bioorg. Chem.* 65 (2016) 126–136.
- [18] S. Naveen, P. Naveen, Zabiulla, H.R. Manjunath, N.K. Lokanath, S.A. Khanum, I. Warad, Crystal structure of 5-(4-methoxyphenyl)-1,3,4-oxadiazol-2-amine, *IUCRData* (2016) 1–4.
- [19] L. Carpino, A. El-Faham, C. Minor, F. Albericio, Advantageous applications of azabenzotriazole (triazolopyridine)-based coupling reagents to solid-phase peptide synthesis, *J. Chem. Soc. Chem. Commun.* 19 (1994) 201–203.
- [20] O.O. Oyedapo, B.A. Akinpelu, K.F. Akinwunmi, Red blood cell membrane stabilizing potentials of extracts of *Lantana camara* and its fractions, *Int. J. Plant Physiol. Biochem.* 2 (2010) 46–51.
- [21] M. Marchesan, D.H. Paper, S. Hose, G. Franz, Investigation of the antiinflammatory activity of liquid extracts of *Plantago lanceolata*, *Phytother. Res.* 12 (1998) 56–78.
- [22] Z. Xu, J. Zhou, J. Cai, Z. Zhu, X. Sun, C. Jiang, Anti-inflammation effects of hydrogen saline in LPS activated macrophages and carrageenan induced paw oedema, *J. Inflamm.* 9 (2012) 21–30.
- [23] S.J. Klebanoff, Myeloperoxidase, *Proc. Assoc. Am. Phys.* 111 (1999) 383–398.
- [24] Klinke, C. Nussbaum, L. Kubala, K. Friedrichs, T.K. Rudolph, V. Rudolph, H.J. Paust, S. Schroder, D. Benten, D. Lau, K. Szocs, P.G. Furtmuller, P. Heeringa, K. Sydow, H.J. Duchstein, H. Ehmke, U. Schumacher, T. Meinertz, M. Sperandio, S. Baldus, Myeloperoxidase attracts neutrophils by physical forces, *Blood* 117 (2011) 1350–1362.
- [25] T.G. Brock, R.W. McNish, M. Peters-Golden, Arachidonic acid is preferentially metabolized by cyclooxygenase-2 to prostacyclin and prostaglandin E2, *J. Biol. Chem.* 274 (1999) 11660–11666.
- [26] Y. Zheng, J. Li, N. Zhao, W. Wei, Y. Sun, One-pot synthesis of mesostructured AISBA-15-SO₃H effective catalysts for the esterification of salicylic acid with dimethyl carbonate, *Microporous Mesoporous Mater.* 92 (2006) 195–200.
- [27] P. Naveen, S. Naveen, Zabiulla, S.B. Benaka Prasad, N.K. Lokanath, S.A. Khanum, I. Warade, Methyl 2-(benzoyloxy)benzoate, *IUCRData* (2016) 1–4.
- [28] P. Naveen, N.D. Rekha, V. Lakshmi Ranganatha, B. Begum, S.A. Khanum, Synthesis of Salicylic acid fused dihydropyrazole analogues and their mechanism of action on *Escherichia coli* cells, *Der Pharma Chem.* 16 (2017) 91–97.
- [29] T. Prashanth, V. Lakshmi Ranganatha, P. Naveen, M. Al-Ghorbani, A. Bushra Begum, S.A. Khanum, Synthesis of (4-benzoyl-phenoxy)-acetic acid and derivatives and their efficacy as antioxidant agents, *Free Radic. Antioxid.* 3 (2013) 550–554.
- [30] V. Kardile, U.B. Mahajan, H.M. Shaikh, S.N. Goyal, C.R. Patil, Membrane stabilization assay for anti-inflammatory activity yields false positive results for samples containing traces of ethanol and methanol, *World J. Pharm. Pharm. Sci.* 5 (2016) 493–497.
- [31] L. Yao, Z. Li, W. Su, Y. Li, M. Lin, W. Zhang, Y. Liu, Q. Wan, D. Liang, Role of mesenchymal stem cells on cornea wound healing induced by acute alkali burn, *PLoS One* 7 (2012) 30842–30867.
- [32] O.O. Adeyemi, S.O. Okpo, O.O. Ogunti, Analgesic and anti-inflammatory effects of the aqueous extract of leaves of *Persea americana* Mill (Lauraceae), *Fitoterapia* 5 (2002) 375–380.
- [33] B. Pulli, M. Ali, R. Forghani, S. Schob, K.L.C. Hsieh, Wojtkiewicz, J.W. Chen, Measuring myeloperoxidase activity in biological samples, *PLoS One* 8 (2013) 67976–67988.
- [34] N. Puttaswamy, G.P. Kumar, M. Al-Ghorbani, V. Vigneshwaran, B.T. Prabhakar, S.A. Khanum, Synthesis and biological evaluation of salicylic acid conjugated isoxazoline analogues on immune cell proliferation and angiogenesis, *Eur. J. Med. Chem.* 114 (2016) 153–161.